REVIEW

A review on plant derived carbon quantum dots for bio-imaging

Ashok Kumar S., [ab] Dheeraj Kumar M.,[b] Mowsam Saikia,[b] Renuga Devi N.[bc] and Subramania A. (ID) *[b]

Carbon quantum dots (CQDs) have emerged as a potent competent to classical metal-based semiconductor quantum dots owing to their fascinating characteristics, such as high biocompatible nature, high solubility in water, excellent chemical stability, low toxicity, surface passivation, remarkable conductivity, and tunable optical characteristics. Such exceptional properties of CQDs prevail in their application as bio-imaging probes. Despite expensive protocols and environmentally threatening processes, research is focused on utilizing CQDs via a green synthesis approach. The present review summarizes the development of plant derived CQDs and their synthesis methods, modification strategies, characterization techniques, properties, and the application of CQDs for advanced bio-imaging applications.

1. Introduction

In the current scenario, immense attention has been paid towards synthesizing QDs for multifunctional applications. The QDs are classified specifically on the basis of their architectural and material diversity. QDs can be classified into perovskite-based QDs, core–shell QDs, magnetic QDs, metal

[a] Dept. of Biomedical Engineering, Saveetha Engineering College (Autonomous), Chennai – 602105, India

[b] Centre for Nanoscience and Technology, Pondicherry University, Puducherry, 605014, India. E-mail: a.subramania@gmail.com

[c] Department of Zoology, G.T.N. Arts College (Autonomous), Dindigul – 624 005, India

dichalcogenide-based QDs, and carbon-based QDs, as depicted in Fig. 1. Perovskite-based QDs have been hotly pursued in current semiconductors owing to their quantum confinement effect and defect-tolerant nature. These QDs inherit the perovskite crystal structure with the chemical formula ABX_3. In ABX_3, A refers to the cations such as Cs^+ methylammonium (MA^+) or formamidine (FA^+), B mainly refers to divalent metals such as Pb^{2+}, Sn^{2+}, Cu^{2+}, Ni^{2+}, Co^{2+}, or Mn^{2+}, and X refers to halogens (I^-, Br^-, or Cl^-).[1] Excellent optical properties of perovskite quantum dots, such as high photoluminescence quantum yield approaching unity, narrow emission bandwidth, and tunable wavelength covering the entire visible spectrum, serves perovskite QDs for their application in next-generation optoelectronic devices and information displays. Colloidal QDs

Mr Ashok Kumar S. obtained his BE in Bio-Medical Engineering from Saveetha Engineering College (Autonomous) Afflicated to Anna University, Chennai-602105, in May 2023. He did his major project under the supervision of Prof. Subramania Angaiah at the Centre for Nanoscience and Technology, Pondicherry University, Puducherry, India, His research interests focus on the development of bio-sensors, quantum dots for bio-imaging, and anti-cancer bone implants.

Ashok Kumar S.

Dr Dheeraj Kumar Maurya obtained his PhD degree from the Centre for Nanoscience and Technology, Pondicherry University, Puducherry, India, under the supervision of Prof. Subramania Angaiah. His current research interests include the development of electrospun nano-hybrid materials for energy storage devices and humidity sensing.
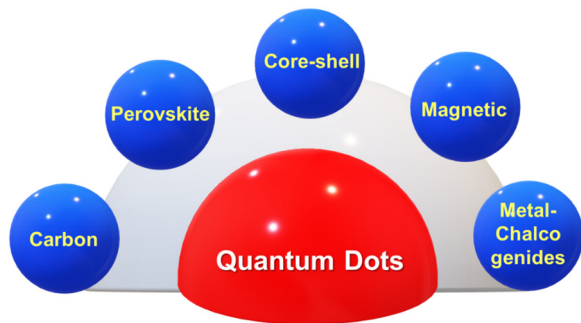
Dheeraj Kumar M.

Fig. 1 Classification of quantum dots.

such as cadmium selenide (CdSe), lead sulfide (PbS), and indium phosphide (InP) are synthesized by suspending semiconductor materials in a suitable solvent and are widely used in display technologies, lighting, and biological imaging applications.[2]

Core–shell QDs are hierarchical structures having a core of one material surrounded by a shell of another material. In these CQDs, the core and the shell are mainly made up of type II–VI, IV–VI, and III–V type semiconductors, such as (CdS) ZnS,

(CdSe) ZnS, (CdSe) CdS, and (InAs) CdSe.[3] These QDs aim toward improving the quantum dot stability, enhancing its photoluminescence and provide better protection against oxidation. Magnetic QDs are basically made from magnetic materials such as iron, zinc, cobalt, or nickel in their specific composition.[4] These quantum dots can exhibit both optical and magnetic properties, making them suitable for applications in spintronics, data storage, and magnetic resonance imaging (MRI).

Metal dichalcogenide quantum dots (QDs) are nanoscale semiconductor materials that consist of metal atoms (such as molybdenum or tungsten) bonded to chalcogen atoms (such as sulfur or selenium) in a layered crystal structure.[5] These quantum dots exhibit unique optical and electronic properties due to their size confinement, which makes them highly attractive for various applications in optoelectronics, photonics, and quantum technologies.[6] Metal dichalcogenides are layered materials with a thickness of only a few atoms. This 2D structure gives rise to unique properties, such as quantum confinement and strong excitonic effects. These properties are of interest for applications in quantum computing, information storage, and spintronics. These QDs can be functionalized with biomolecules to enable specific targeting and imaging biological systems. Their small size, biocompatibility, and bright emission make them valuable tools for bioimaging and biosensing applications. The also have an ability to undergo redox reactions that make them suitable for supercapacitors and batteries, where they can enhance energy storage capacity and cycling stability.

Carbon quantum dots (CQDs) are typical zero-dimensional quasi-spherical shaped crystalline nanoparticles with ultra-small sizes (less than 10 nm) exhibiting quantum confinement effect. CQDs mainly possess a sp^2 conjugated core and contain oxygen content in the form of multiple oxygen-containing species represented by several functional groups like ether, carboxyl, epoxy, hydroxyl, and aldehyde groups.[7,8] CQDs are composed of carbon based materials such as graphene and

Mr Mowsam Saikia is currently pursuing his PhD at the Centre for Nanoscience and Technology, Pondicherry University, Puducherry, India, under the supervision of Prof. Subramania Angaiah. He received his MSc in Biotechnology from Bangalore University. His research interests focus on the development of anti-cancer bone implants, bio-imaging, and bio-sensing.

Mowsam Saikia

Dr Renuga Devi Navaneethan, is working as the Head & Associate Professor at the Dept. of Zoology at the G.T.N. Arts College, Dindigul, India. She is a recipient of the INSA Fellowship and worked under the guidance of Prof. Subramania Angaiah, at the Centre for Nanoscience and Technology, Pondicherry University, India. Her current research includes the synthesis of inorganic and carbon quantum dots for bio-medical applications, metagenomics, environmental biotechnology and microbiology.

Renuga Devi N.

Dr Subramania Angaiah is a Professor at the Centre for Nanoscience and Technology, Pondicherry University, India. He did his Post-doctoral research at KIST, South Korea. His current research interests include the development of nanostructured materials for energy, medical, and environmental applications.
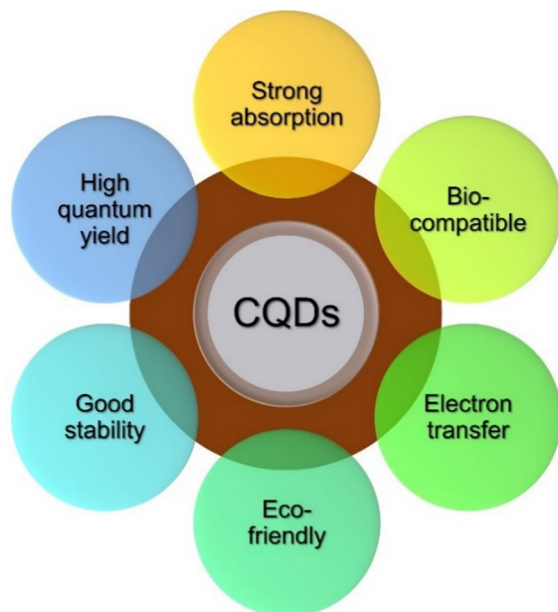
Subramania A.

Fig. 2 Properties of CQDs.

carbon nanotubes. They have unique optical and electronic properties. They have potential applications in bioimaging, sensors, and optoelectronic devices. They have remarkable properties, such as high electron conductivity, outstanding water solubility, high photoluminescent quantum yield, fluorescence property, tunable excitation, emission characteristics, enhanced electro-catalytic activity, low toxicity, high solubility, excellent biocompatibility, and long-term chemical stability (Fig. 2).[9,10]

In recent years, green synthesis routes for synthesis of CQDs are highly preferred over chemical methods due to their superiority in terms of chemical exposure, simple synthesis protocols, low cost, sustainability, non-toxicity, eco-friendliness, and cost-effectiveness.[11,12] Interestingly, the precursors for green synthesis are highly abundant in the earth in the form of plants. Plant parts, including root, stem, leaf, fruit, flower, and seed, have been used in the synthesis of green CQDs. These precursors are cheap, safer, highly abundant, and environmentally friendly as compared to others. Plant precursor-based synthesis does not need a separate reactant for doping, surface passivation, or post modification due to the inevitable presence of carbohydrates, proteins, amino acids, and other biomolecules, which provide sufficient elements for the surface functionality of CQDs.

CQDs have gained significant attention in the field of bioimaging due to their unique properties and advantages over other quantum dots (QDs) made from different materials. CQDs exhibit high biocompatibility than semiconductor-based quantum dots. The demands of biocompatibility and hydrophilicity are highly urged in biological applications, including bioimaging. CQDs are highly water soluble and are capable of dispersing in all biological media. This hydrophilicity stabilizes CQDs as a potential candidate for labeling and

imaging biological samples without additional modifications. CQDs offer excellent size tunability, enabling precise control over their physical and optical properties. By adjusting the synthesis parameters, such as reaction time or precursor concentration, the size of CQDs can be tailored to optimize their photoluminescent properties for specific bioimaging applications. These QDs exhibit excellent photoluminescent properties, including high quantum yield, tunable emission wavelengths, and high photostability. These properties make them ideal for fluorescence-based bioimaging, where they can be used as bright and stable probes for visualizing biological structures and processes. Compared to other types of QDs, the synthesis of CQDs is generally straightforward, cost-effective, and environmentally friendly. Carbon-based precursors, such as citric acid or glucose, are readily available and relatively inexpensive, allowing for large-scale production of CQDs. Carbon quantum dots can be easily functionalized with various biomolecules, such as antibodies, peptides, or targeting ligands, to achieve specific targeting and imaging biological targets. This versatility allows for the development of targeted bioimaging probes with enhanced specificity and sensitivity. CQDs exhibit good stability under physiological conditions, maintaining their optical properties over time. They are less prone to photobleaching and degradation compared to some other types of quantum dots, ensuring reliable and long-lasting imaging results. These advantages position carbon quantum dots as promising candidates for bioimaging applications, offering a combination of biocompatibility, water solubility, tunable optical properties, cost-effectiveness, and functionalization versatility that make them highly attractive in the field of biomedical imaging.

Further, carbon dots are classified into graphene quantum dots (GQDs), carbon quantum dots (CQDs), carbon nanodots (CNDs), and carbonized polymer dots (CPDs) on the basis of their formation mechanism, micro-/nanostructures, chemical structure, and morphology.[7,13] GQDs refers to the single or multilayer graphite structures possessing chemical moieties or functional groups on the surface/edge or interlayer spacing. These GQDs are prepared through the top-down method that involves the breakdown of carbonaceous precursors (carbon fibers, carbon rods, carbon nanotube, graphite powder, and carbon black) into small pieces. The optical properties of GQDs are dominated by the size of π-conjugated domains and the surface/edge structures.[14] In terms of morphology, CQDs, CNDs, and CPDs are spherical structures, whereas GQDs display anisotropy with lateral dimensions larger than their height. In contrast with GQDs, the synthesis of CQDs and CPDs is done *via* bottom-up approaches in the form of different processing treatments, such as assembly, polymerization, chemical crosslinking, and carbonization. CQDs are crystalline and inherit a large number of chemical functionalities that impart the intrinsic state luminescence and quantum confinement phenomenon. CNDs are amorphous quasi-spherical dots that do not exhibit the quantum confinement phenomenon. In the amorphous graphitic sp^2 structures of CNDs, the near-UV to blue emission is observed. This emission is anticipated to be the recombination of the photogenerated electron–hole pairs. Notably, CPDs are the crosslinked nanohybrid and carbonized

polymer hybrid structures of carbon and aggregated polymers, having a carbonized core at the center enveloped by either the polymeric chains or functional groups. CPDs exhibit higher stability, better compatibility, easier modification, and functionalization.[15] The molecular state and crosslinked enhanced emission effect in CPDs are responsible for the optical characteristics of CPDs.

This review gives a brief overview of carbon quantum dots mainly derived from plant precursors. Initially, the prominent synthesis approaches for synthesis of CQDs is discussed and then modification strategies, characterization, and properties of CQDs are also discussed. The role of these CQDs on their application in bioimaging is critically reviewed.

2. Synthesis of plant derived CQDs

There are various methods reported for the synthesis of plant-derived CQDs, mainly comprising top-down (cutting larger carbon materials) and bottom-up (fusing small precursor materials) approaches. The top-down approach of CQDs involves arc discharge, laser ablation, chemical ablation, electrochemical carbonization, and ultrasonic synthesis, whereas bottom-up synthesis comprises thermal decomposition, microwave pyrolysis, chemical oxidation, hydrothermal/solvothermal process, pyrolysis template, and plasma treatment.[16–20] Bottom-up approach is widely adopted over bottom-up methods owing to its high yield. The most preferable methods for the synthesis of plant derived CQDs are shown in Fig. 3.

2.1 Hydrothermal method

The hydrothermal method is one of the simple, affordable, and environmentally beneficial ways of synthesizing CQDs from natural sources. This process encompasses all four significant processes involved in synthesizing CQDs: carbonization, dehydration, passivation, and polymerization.[7,22] Typically, the precursors and suitable solvent are mixed and sealed in the Teflon-lined autoclave at elevated pressure and heated at high

temperatures for several hours. The heating temperature is usually maintained between 150 °C to 250 °C. As a result, the color of the solution changes to brown or yellow, indicating the formation of CQDs. In addition, the particle shape, surface chemistry, and crystalline phase can be tailored by adjusting the temperature, pressure, solvent, and reaction time. However, the CQDs obtained are not of uniform size and require filtration for uniform-size distribution. For example, Gopinath Packirisamy et al. reported the synthesis of CQDs with better solubility, biocompatibility, quantum yield, and chemical stability as bioimaging agents for the sensing of metal ions. However, the enhanced properties arise due to the passivation of CQDs by oligoethyleneamine. Further, on insertion as a biolabeling agent into Zebrafish embryos, the CQDs display better fluorescence in green, followed by blue and red as an alternative for contrasting probes.[23] As a step forward, Divya Ottoor et al. synthesized CQDs from groundnuts by facile and effective hydrothermal carbonization as a bioimaging agent for the imaging of MCF breast cancer cells. At the end of bioimaging studies, the CQDs did not show an apparent change in morphology and shape, proving their efficiency for bioimaging applications.[24] Nagappan Rajendiran et al. synthesized CQDs from sweet corn (Zea mays L. var. rugosa) as a fluorescent probe for imaging of A549 cells. As an outcome, the in vitro hemolytic assay and ESR estimation demonstrated that the prepared CQDs had good hemocompatibility properties at 250 g mL^{-1} concentration on human RBCs.[25] Similarly, Aschalew Tadesse synthesized nitrogen-doped carbon quantum dots from lemon with better photo fluorescence properties for bioimaging applications. On investigation, the NCQDs display high quantum yield, better fluorescence properties, stability, and better biocompatibility serving as an essential candidate for in vitro and in vivo imaging applications.[26]

2.2 Microwave method

Microwave treatment is a streamlined, scalable, low-cost, eco-friendly, and rapid way to produce CQDs. Microwave radiation
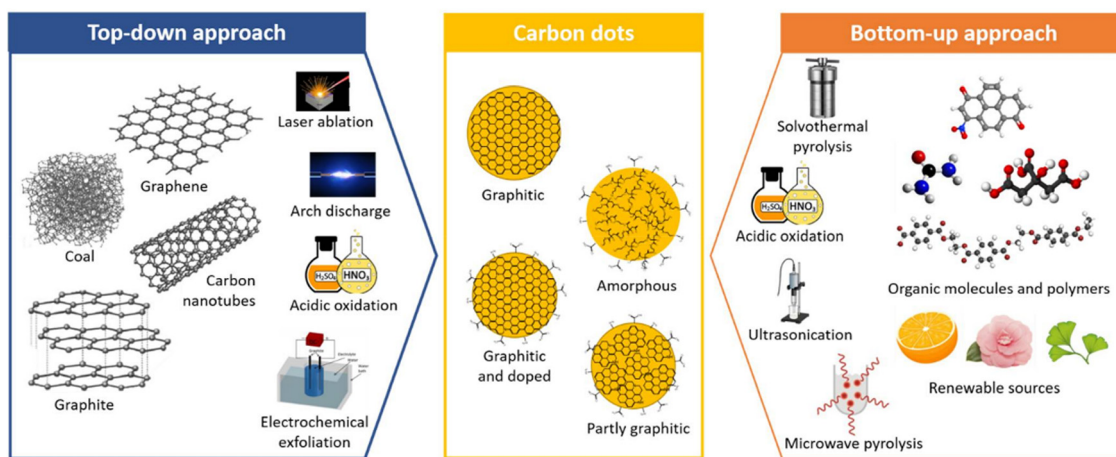

Fig. 3 Different approaches for synthesis of CQDs. Figure is reproduced from the ref. 21 under Copyright © 2022 Creative Commons Attribution (CC BY) license.

offers fast *in situ* temporary heating, producing high-quality CQDs and reproducibility. This method involves exposing a reaction mixture containing carbon precursors to electromagnetic radiation, usually within 1 mm to 1 m. The microwave chamber is uniformly heated due to the electromagnetic waves being converted to thermal energy. The generation of the microwave effect arises due to the material-wave interaction and dipolar polarization of molecules in the solution. Following irradiation, the molecules reorient, which causes collisions and a rise in solution temperature. The polarity of the reacting molecules has a significant impact on the efficiency of this method. Though microwave heating is an efficient method for synthesizing CQDs from a plant source, solvents with high boiling points cannot be used. For example, Feitosa *et al.* synthesized CQDs by microwave-assisted method from cashew gum through a two-step process involving depolymerization and carbonizations for its application in bioimaging.[27] As a step forward, Milan Kumar Bera *et al.* synthesized CQDs with a size range of 2.7 nm to 10.4 nm from the leaf of calotropis gigantea (crown flower) by the microwave-assisted method. The synthesized CQDs work efficiently as a fluorescent agent for biolabeling bacteria and viruses.[28] Similarly, Architha *et al.* developed fluorescent CQDs for bioimaging applications employing Mexican mint leave as precursors,[29] as shown in Fig. 4.

2.3 Chemical oxidation method

Chemical Oxidation is the most common top-down route for preparing CQDs because of various advantages such as high yield, high purity, low cost, and reasonable control over the size. It is used to exfoliate and break down large chunks of carbon into smaller pieces while simultaneously adding hydrophilic groups like hydroxyl (–OH) or carboxyl (–COOH) groups that could improve the water dispersion and FL characteristics of the resulting particles. The oxidants such as HNO_3, phosphoric acid (H_3PO_4), and sulfuric acid (H_2SO_4) are used to facilitate the carbonization of plant parts to get CDs, as shown in Fig. 5. In most cases, the parts of the plant are first carbonized, then combined with a chemical oxidant, followed by separation and purification operations. Thus, producing CQDs using the chemical oxidation approach is simple, scalable, and does not require expensive equipment. Gunjal *et al.* prepared CQDs by oxidizing mahogany fruit shell powder using H_2SO_4 and HNO_3. By adequately combining dried shell powder with concentrated H_2SO_4 and neutralizing, activated carbon was formed from the mahogany fruit shell. The mixture of 50 mL of 1.0 M HNO_3 solution and 0.5 g of activated carbon was then sonicated for 10 min. After sonication, the mixture was subjected to reflux for 12 h, causing a colour change to brownish yellow, symbolizing the formation of CQDs. The sodium carbonate (Na_2CO_3) served as a neutralizing agent.

For example, Kailasa *et al.* synthesized mutlicolour emissive carbon dots, namely B-, G-, and Y-CMCDs, from muskmelon by employing different oxidizing agents and tuning the reaction parameters. Fig. 5 represents the fabrication of multicolor-emissive CDs from muskmelon. The synthesized CQDs were tested on *Cunninghamella elegans*, *Aspergillus flavus*, and

Fig. 4 Synthesis process of CQDs by microwave method reproduced with permission from ref. 29 Copyright © 2021 Elsevier.
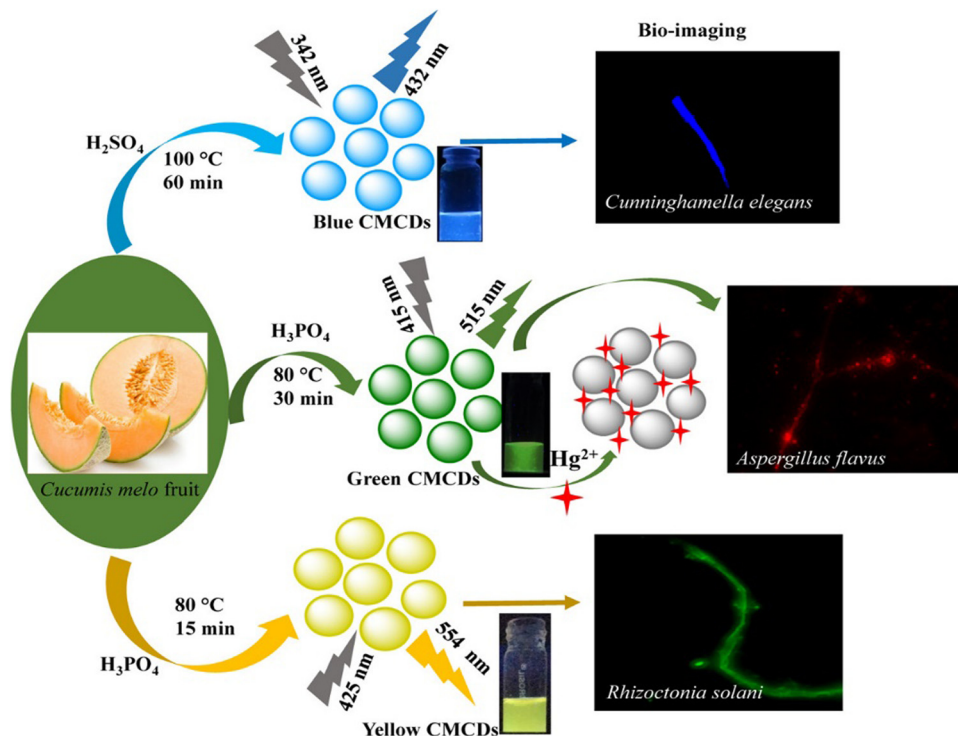
Fig. 5 The fabrication of multicolor–emissive CDs from muskmelon. The figure is reproduced with permission from ref. 30 under Creative Common License Copyright © 2019 American Chemical Society.

Rhizoctonia solani cells, exhibiting better nontoxicity and bio-compatibility, proving an excellent fluorescent probe for imaging purposes.[30]

2.4 Pyrolysis method

The pyrolysis technique is simple and economical for the bulk production of carbon dots. In this technique, the materials are subjected to heat in the presence of controlled pressure above the melting point in the absence of oxygen. Under this atmosphere, physical and chemical changes occur in organic precursor substances, resulting in carbon-containing solid residues. CQDs are, in general, obtained after further condensation and nucleation. Pyrolysis treatment is a well-known method for producing CQDs. It is an irreversible thermal decomposition reaction in which the plant part materials decompose in an inert atmosphere. It involves physical and chemical changes in materials, producing solid black carbon residue. This method has the benefits of being rapid, simple, and eco-friendly, but it is difficult to scale up and produces a broad size distribution. Commonly, pyrolysis is performed at very high temperatures and under controlled pressure, forming black carbon materials that can be separated and purified to obtain the CQDs.

By pyrolyzing the watermelon peels at low temperatures and filtering the mixture, Zhou *et al.* synthesized CQDs on a large scale. The produced C-dots exhibit strong blue luminescence, excellent water solubility, and good stability in a wide range of pH solutions and high salinity solutions. As an outcome, the obtained CQDs were used to image HeLa cell lines.[31]

Meanwhile, by pyrolyzing lychee seeds, fluorescent CQDs were synthesized with a quantum yield of 10.6% and used for imaging Hep G2 cells.[32] In addition to lychee seed, lychee exocarp was also employed to synthesize CQDs. Due to their better compatibility and fluorescent property, the obtained CQDs serves as an excellent nanoprobe for imaging of cancer cells.[33] Similarly, Liangliang Zhang utilized peanut shells as a precursor for synthesizing CQDS by pyrolysis method for multi-color imaging of living cells. The produced C-dots exhibit excellent stability, high fluorescence luminescence, good water solubility, and good resistance to photobleaching, ionic strength, and pH changes.[34] Table 1 shows different methods for the synthesis of CQDs from various plants.

3. Modification strategies for CQDs characteristics

3.1 Tuning the shape and size

The size-dependent PL emission has been prominent in CQDs due to quantum confinement effects. Tuning the shape and size is highly desired for characteristic applications. The optical band gap of CQDs is determined by size and shape, along with the fraction of the sp^2–sp^3 hybridized domains. Until now, precise control of the CQDs' size below 5 nm has been difficult to implement.[9,18] Currently, shape and size tuning is practiced *via* the adoption of preparation and post-preparation treatment such as filtration, dialysis, centrifugation, column chromatography, and gel-electrophoresis. Confined pyrolysis is an

Table 1 Different methods for the synthesis of CQDs from various plants

Plant name	Parts used	Size (nm)	Synthesis method	Applications	Ref.
Seawood			Hydrothermal	Toxicological effects	35
Azadirachta indica, *Ocimum tenuiflorum*, *Tridax procumbens*	Leaves	6–12	Chemical oxidation	*In vitro* cell imaging	36
Watermelon Peel	Fruit	2.0	Carbonization	Live cell imaging	31
Mangifera indica	Leaves	1–5	Pyrolysis	Detection of metal ions	37
Calotropis gigantea (crown flower)	Leaves	2.7 to 10.4	Microwave-assisted synthesis	Bio-imaging of bacteria, fungi and plant cell	38
Catharanthusroseus (white flowering plant)	Leaves		Hydrothermal	Detection of multi-ions	39
Spinach	Leaves	5.6 nm	Hydrothermal	Fe^{2+} detection	40
Plectranthus amboinicus	Leaves	2.43 ± 0.02	Microwave-assisted synthesis	Bioimaging	29
Phoenix dactylifera	Leaves	5–15	Hydrothermal	Cell imaging	41
Sweet corn		<2.4	Hydrothermal	Bioimaging	42
Coriander	Leaves	1.5–2.98	Hydrothermal	Bioimaging	43
Cydonia oblonga	Fruit	4.85	Microwave-assisted synthesis	Cell imaging	44
Groundnut	Seed	2.5	Hydrothermal	bioimaging of MCF-7 cells	24
Manilkara zapota	Fruit	—	Hydrothermal	Imaging of cells	45
Citrus lemon	Fruit juice	1–6	Hydrothermal	Imaging of cells	26

effective strategy to tune and obtain uniform sizes of CQDs using an organic precursor in nanoreactors *via* three steps. (i) absorbing the organic precursor into porous nanoreactors *via* capillary force (ii) pyrolysis of the organic precursor confined in the nanoreactors into carbonaceous matter, (iii) release of the as-synthesized CQDs by removing the nanoreactors. Porous silica and core shell nanoparticles are widely employed nanoreactors for this technique, whereas thermally unstable polymers are employed as block matter to overcome the aggregated carbonaceous entities during thermal treatment.

3.2 Elemental doping

Fluorescent properties can be finely tuned *via* heteroatom doping (metals/non-metals) in CQDs. Elements such as nitrogen (N), sulfur (S), boron (B), phosphorus (P), fluorine (F), and silicon (Si) are highly preferred for elemental doping in CQDs *via* post-treatment processes.[16,46,47] The nature and bonding configuration of doped heteroatoms highly influences the physicochemical preparation of CQDs. Heteroatom doping in CQDs not only avails the more reactive but is also added to the carbon network of CQDs to tune the initial band gap and establish new energy levels. Namely, heteroatom doping enables alteration of the electron orbital region of sp^3 hybridization in the carbon core as well as sp^2 hybridization on the surface. It endows CQDs with bandgap narrowing, wider light absorption, and higher QYs. The energy gap between the π orbital of O, N, and S and the n orbital of C reduces in turn. After doping elements such as N and S, the energy required for electron transition from the π orbital of C–O, C–N, and C–S to the n orbital is lower, which can greatly improve the fluorescence QYs of doped CQDs. N ($1s^2 2s^2 2p^3$) adjacent to C ($1s^2 2s^2 2p^2$) in the periodic table is the most widely used element for heteroatom doping of CQDs. N possesses five valence electrons and is facile to bond with C. Additionally, N exhibits a stronger

electronegativity of 3.04 than that of C (2.55). Thus, N is inclined to embed into the carbon network through substituting C. N-Doping can introduce the disturbance of the surrounding electronic environment, create new radiation composite pathways, and thus adjust the band structure. The doping mechanism mainly involves the study of the doping amount and bonding configurations. In principle, the fluorescence performance of doped CQDs has a positive correlation to the doping amount.

3.3 Surface modification

Surface modification plays an intermittent role in tuning the surface characteristics for specific applications. Functionalization in the surface of CQDs can be done through surface chemistry like covalent bonding, coordination, p–p interactions, and sol–gel technology.[7,11,48] Presence of oxygen rich species in CQDs enables them to form covalent bonding. Surface passivation *via* covalent bonding of amine-containing agents extensively improves the photoluminescence of CQDs.[49]

4. Characterization of CQDs

Quantum dots often present superior traits in terms of structural, chemical, and optical characteristics from their bulk counterparts, *i.e.*, nanoparticles. This enables them to be precisely investigated through various characterization techniques and analysis protocols for their diverse applications.[50] Plant derived CQDs are characterized through microscopy, spectroscopy, diffraction, and mass spectrometry based on fundamental techniques. The involved techniques and the obtained information from different characterization techniques are tabulated in Table 2.

Table 2 Different characterization techniques involved in the detailed characterization of plant derived CQDs and acquired information

Characterization	Technique	Information
Microscopic	Atomic force microscopy (AFM)	Topographical
	Scanning electron microscopy (SEM)	Surface morphology
	Transmission electron microscopy (TEM)	Morphology, composition, and crystallographic information
Spectroscopy	Photoluminescence (PL) spectroscopy	Optical characteristics, Quantum yield estimation
	Ultraviolet-visible (UV-VIS) absorption spectroscopy	Identification of electronic transition bands
	Infrared (IR) spectroscopy	Chemical functionalities, structural composition
	Raman spectroscopy	Chemical structure, phase, molecular interaction
	Energy dispersive spectroscopy (EDS)	Elemental composition
	Nuclear magnetic resonance (NMR) spectroscopy	Chemical bond formations, elemental composition, identification of functional group
	X-Ray photoelectron spectroscopy (XPS)	Electronic state of elements
Diffraction	X-Ray diffraction (XRD) analysis	Crystallinity, phase purity, particle size
Scattering	Dynamic light scattering (DLS) analysis	Particle size distribution
	Small/wide-angle X-ray scattering	Averaged particle size, shape, distribution, surface to volume ratio
Stability	Zeta potential measurement	Stability of quantum dots
Mass spectrometry	Electrospray ionization Quadrupole time-of-flight tandem mass spectrometry	Elucidation of the chemical structures of desired nanosized quantum dots
	Matrix-assisted laser desorption/ionization time-of-flight mass spectrometry	

5. Properties of CQDs

5.1 Optical properties

CQDs have attracted tremendous interest in recent years due to their exceptional characteristics, such as low toxicity, small size, ease in functionalization, eco-friendly synthesis, and diverse imaging capabilities. However, the insights of optical characteristics play a vital role in determining the application oriented tunability of CQDs. Understanding the optical properties of CQDs is of great significance for the controllable development of top-designed CQDs with functional purposes.

5.1.1 Absorbance. Absorbance plays a vital role in characterizing CQDs for diverse applications. CQDs synthesized using different synthesis methods exhibit characteristic absorption curves. In general, CQDs show a strong absorbance in the ultraviolet region, *i.e.*, 200–400 nm, accompanied by a tail into the visible light spectrum, *i.e.*, 400–700 nm. The strong absorption peak observed at 230 nm is assigned to the π–π^* transition of C=C, whereas the shoulder peak at 300 nm is assigned to the n–π^* transition of the C=O/C=N bond. It is widely stated that absorption characteristics of CQDs are highly influenced by the types and content of surface groups, size of π-conjugated domains, and variation in the concentration of the oxygen/nitrogen content in carbon cores. Different practices have been adopted to tune the absorbance characteristics of CQDs. For example, surface engineering of CQDs alters their absorption as well as emission spectra, and heteroatom doping regulates absorption characteristics due to their alteration in the π–π^* energy levels and induction of surface defects.

5.1.2 Photoluminescence. Interestingly, photoluminescence (PL) is the most appealing property of CQDs that exhibits excitation-dependent luminescence spectra from ultra-violet to visible to near infrared region. The PL characteristics can be extensively tuned by altering the excitation wavelength involving the quantum confinement effect. Multi spectra can be obtained from a single CQD by varying excitation wavelengths without changing the chemical structure or size. In general,

CQDs exhibit PL spectra in blue and green regions. Acquisition of this phenomenon in red and NIR can be achieved by optimizing reaction parameters and precursors for carbon. This spectrum can be tuned by surface engineering, varying the initial precursors, and synthetic methodologies for CQD synthesis. In certain cases, CQDs exhibit up conversion PL, where the peak maxima in emission spectra appear at the shorter wavelength when subjected to excitation using a longer wavelength. This optical phenomenon serves CQDs as a potential contender for *in vivo* bioimaging with improved photon tissue penetration, reduced background autofluorescence, and low photon-induced toxicity at longer wavelengths in the NIR region.

5.1.3 Quantum yield. Quantum yield (QY) is also one of the vital parameters of CQDs for their applications in photodevices. QY mainly refers to the ratio of the number of photons emitted to those absorbed by the CQDs.[7,8,50] Tremendous efforts have been laid by the researchers in further enhancing the QY of CQDs, which is a prerequisite for its applications. This can be achieved by practicing surface modification and heteroatom doping in CQDs. Surface modification effectively transforms the electron withdrawing group into electron donating group without any sacrificial shape of the carbon nanostructure. On the other hand, heteroatom doping lead to the alteration in bandgap and characteristic electron densities that increases the QY of CQDs.

5.1.4 Phosphorescence. Ambient temperature phosphorescence is a fascinating characteristic of CQDs owing to the intersystem transition from the lowest excited singlet state to a triplet state and radiative transition from the lowest excited triplet state to the ground state. The first aims to facilitate the intersystem crossing ability by enriching the spin–orbit coupling by transition metals, while the second involves suppression of non-radiative transitions by restricting rotation and vibration.[51] These two processes are crucial for generating ambient temperature phosphorescence from organics. This can be achieved by employing CQDs with enormously cross-linked structures containing non-conjugated groups (C=O and

C=N) due to their strong spin–orbit coupling and heteroatom doping (N, P *etc.*) that promotes the n–π* transition of C=O and C=N favouring ambient temperature phosphorescence.

5.1.5 Chemiluminescence. Chemiluminescence (CL) mainly refers to the generation of light through a chemical reaction. CQDs exhibit the CL phenomenon when dissolved in aqueous solvents *via* redox reaction with the formation of unstable products from intermediate radicals.[22,49] The CL in CQDs is possibly accredited to either three reasons, *i.e.*, (1) excitation after direct oxidation, (2) through the enhancement, and (3) inhibition of their luminescence. Additionally, CQDs are capable of emitting photons in the visible region when subjected to electrically induced excitation, commonly referred to as electrochemiluminescence.

5.2 Electrochemical properties

CQDs are highly preferred over other carbon-based nanomaterials owing to their low toxicity, cheaper cost, and eco-friendliness. The presence of chemical moieties like hydroxyl, carboxyl, and amine functional groups on the surface of CQDs enables a high density of active sites for surface modifications, which is highly beneficial in electrocatalytic activity.[48] Capability of being doped by N, P, S, and B enables CQDs in intra-molecular charge transferability *via* improvement in electronic traits of CQDs. The heteroatom-doped CQDs exhibit exceptional electrochemical performance due to the enhancement of intrinsic activity of surface functional sites, distortion of their electronic configuration, tuning of local densities, as well as the acceleration of adsorption and desorption phenomena.

5.3 Biological properties of CQDs

The carbon quantum dots (CQDs) are a novel, nanostructured carbon-based material with a strong emission fluorescence. Ultrafine particles smaller than 10 nm in size compose this one-of-a-kind, quasi-spherical carbon nanoparticles.[52] In 2004, during the purification of single-walled carbon nanotubes, CQDs were initially identified as a component of luminous nanoparticles. Sun *et al.* suggested a method to create CQDs by straightforward surface passivation and chemical modification for increasing fluorescence emission.[53] It is commonly accepted that CQDs follow the core/shell concept, with the carbon core consisting of graphitic pieces and the shell consisting of different surface functional groups. Conjugated chromophore fragments from the core and/or surface contribute to the luminescence.[54] CQDs are one of the recently discovered allotropes of carbon, and they have several useful properties. These include minimal cytotoxicity, strong biocompatibility, persistent chemical inertness, efficient light harvesting, and amazing photoinduced electron transfer. CQDs are promising candidates for a wide range of applications in biosensors, such as electron transfer-based detection of copper ions in living cells.[55–57] These zero-dimensional, spherical, water-soluble nanoparticles have variable luminescence and are photostable, making them an exciting scaffold for use in biomedical, photocatalytic, and sensing applications.[58] CQDs have potential applications in biosensor, green reductant, and

biomarker, bioimaging,[59,60] optoelectronic devices,[61] *etc.* The biological property of carbon dots depends on the source from where it is derived. Generally, the biomass derived carbon dots are known for biocompatibility as their size is too small and are made of carbon core formed from biomass. The biomass derived carbon dots can also be an excellent vector for drug delivery because of their excellent biocompatibility and the capability to pass through the cell membrane, and also show an exceptional biocompatibility as high as 15 mg mL^{-1} concentration.[62] BCQD can be tracked while we try to tag a particular substrate due to its excellent fluorescent property, which will, in turn, help us to track the drug delivery process and will be able to confirm that the targeted drug is delivered to the correct position. As a result of their high photocatalytic activity, CQDs have found widespread use in the photocatalytic area. One example is the visible-light-responsive CQDs made from pear juice and used to effectively degrade methylene blue by Kim *et al.*[53,63] CQDs have been explored as biocompatible fluorescent dyes for *in vivo* imaging as an alternative to carrying drug molecules due to their low or non-toxicity. The photodegradation of CQDs made from various carbon sources cannot be tolerated. CQDs are an excellent option since they may be tailored for PL emission by introducing a wide variety of functional groups.[64–66] Due to the thick background in the NIR "water window," PL emission of CQDs in the NIR region is particularly important and crucial for *in vivo* optical imaging. The CQDs with strong absorptivity can make up for reduced fluorescence yield in bioimaging when compared to other heavy metal QDs. Sun *et al.* originally suggested a method for staining Caco-2 cells using PEG1500N passivated CQDs for cellular imaging, indicating that CQDs can be used in fluorescent labelling of cells.[67] Carbon dots are an excellent source for drug delivery when the carbon dot is made of the same kind of material that we wish to target. In order to examine drug delivery, Ding and colleagues created BCQDs utilizing genomic DNA as a carbon source to target the genomic DNA of cancer cell and deliver it from cytoplasm to nucleus by means of irradiation, as shown in Fig. 6.[53]

5.3.1 Multiphoton imaging. The fluorescent imaging method, known as two-photon excitation microscopy or 2PEF, is very effective for capturing images of scattering living tissues with a thickness of up to one millimetre. Two-photon excitation necessitates simultaneous excitation by two photons with wavelengths greater than the emitted light, in contrast to conventional fluorescence microscopy, where the excitation wavelength is shorter than the emission wavelength. The image is successfully created by scanning the sample with the laser while focusing on a particular spot in the tissue. Two long-wavelength photons, often near-infrared (NIR) photons, are simultaneously absorbed by the luminophore in the well-studied up conversion luminescence process known as two-photon fluorescence (TPF), which results in a short-wavelength emission. TPF imaging enables deeper penetration into bio-tissues by using NIR excitation.[68] The dependence of the observed luminescence intensity on the excitation laser power is used to confirm the two-photon nature of the luminescence
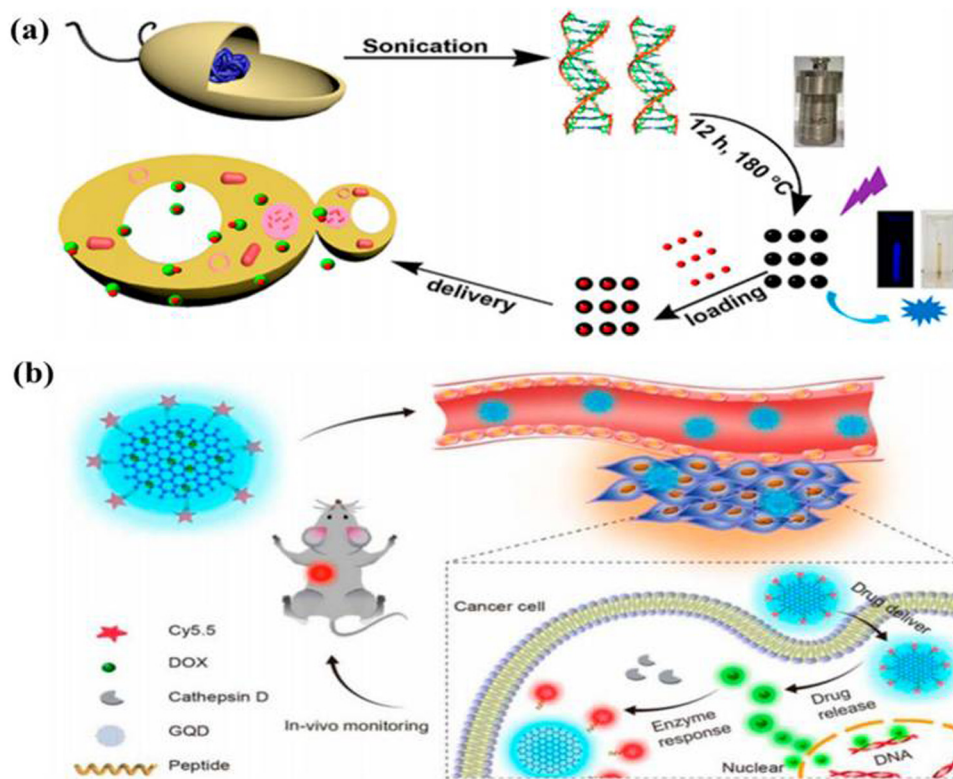
Fig. 6 (a) Diagram showing the creation of DNA-BCQD and its use in drug delivery. (b) Theragnostic agent *in vivo* monitoring strategy using CQDs. Figure is reproduced from ref. 53 under Creative Common CC BY license.

with pulsed infrared laser excitation. The confocal microscope's external detector is used to capture the luminescence signals, and a precision power meter is placed in the focus plane to measure the laser powers for excitation.[69] Due to their intense two-photon activity, C-dots produce dazzling luminosity in the visible when excited by pulsed lasers in the near-infrared. The C-dots' estimated two-photon absorption cross-sections are comparable to those of the top semiconductor quantum dots or core–shell nanoparticles in terms of performance.[69] There have been numerous reports of CQDs with TPF features; however, the majority of these reports relied on the use of NIR-I photons (750–950 nm), particularly the 800 nm excitation, which is still plagued by serious scatter problems for *in vivo* study. NIR-II ($>$1000 nm) excitation with little tissue absorption and the scatter is necessary to further enhance the image quality. However, only a small number of investigations have documented CQDs that effectively exhibit two-photon excitation (TPE) in the NIR-II range.[69–75] It is a promising method for effective *in vivo* multiphoton fluorescence bioimaging, which is a surface modification of CQDs with S–O/C–O groups.[75]

5.3.2 Toxicity. CQDs are typically regarded as extremely biocompatible and secure engineered nanomaterial.[76] Numerous cytotoxicity tests have shown that CDs have very little toxicity (with or without surface passivation) and are easily internalised by cells for imaging.[77] Due to their excellent biocompatibility, CQDs do not significantly alter the pathology

of the organism once they have been ingested and can exit through regular metabolic routes. CQDs have superior biosafety and a higher EC50 (50% effective concentration) for organisms when compared to metal quantum dots.[78] It appears that CDs functionalized with polymers having a neutral surface charge, such as PEG, are the best option for cell labelling without interfering with cellular functions. As a result, this technique would be suitable for *in vivo* imaging. On the other hand, frequently used CDs stabilised with negatively charged COO^- groups should be treated with extreme caution, primarily because they can promote cell proliferation at low concentrations and anomalies in the cell cycle at greater concentrations.[79] Although there have been numerous research works on the toxicity of CQDs, some issues remain. The majority of research only evaluated one form of CQD at a time, and the experimental settings used in each study may have varied. It is challenging to compare the results of different CQDs and studies because there are no common assays to test the toxicity of CQDs. Second, essentially no information exists regarding the long-term effects of CQDs on aquatic species, while the majority of studies have concentrated on the acute toxicity of CQDs.[80]

6. Bioimaging applications of CQDs

Bioimaging is a technique used to monitor the biological process to analyse cell morphology and physiological processes,

and further, it adds to the detection of 3D images of specimens without impairing the numerous life activities such as movement, respiration, *etc.* It is useful in bridging the observation of subcellular structures and all of the tissues in multicellular organisms.[81] The imaging agents should have some basic properties, such as water solubility and non-toxic to species, with advantageous photophysical characteristics, such as significant Stokes shifts, high quantum yields, photo bleach resistance, extended lifetimes, and excitation/emission characteristics suitable for commercially accessible hardware.[82] Based on nanoprobes, luminescent bioimaging has emerged as a potent technique for mapping molecular events and seeing tissues with cellular or sub-cellular resolution. It is highly sensitive, non-invasive, and selective.[83] Since their discovery in 2004, carbon dots (CQDs, which include carbon nanodots, C-dots, carbon quantum dots, and graphene quantum dots in this context) have undergone tremendous development as a result of their distinctive features and exciting potential applications.[54] Since carbon typically makes up most CQDs, they have extremely low cytotoxicity and good biocompatibility. They have a variety of conjugated surface groups, which are advantageous for functionalization for various applications, including use in light-emitting diodes (LEDs), photovoltaic cells, catalysts, fluorescent sensors, bio-imaging agents, and nanomedicines, allowing them to emit multiple colours of light in the visible light region.[84–88] The applications of bioimaging are either done *in vitro* in cell lines or *in vivo*, such as to stain the internal organ or metabolites. Bioimaging of microbes using carbon dots is also an alternative to many corrosive dyes that affect the environment.

6.1 *In vitro* imaging

In vitro bioimaging study utilizes microorganisms, cells, or biological molecules outside of their natural biological context to study the bioimaging property prior to *in vivo* studies. Because we cannot sacrifice a life to our wish, we use animal cell lines that partially imitate the actual cells *in vivo*. So, it is necessary to study any drug that needs to be used for *in vivo* studies to go through *in vitro* studies. Several scientists have explored the area of *in vitro* bioimaging in cell lines from biomass derived carbon dots. Many scientists used biomass derived carbon dots for imaging different cell lines, *e.g.*, HeLa, and it is found that the CQDs generally stain the cytoplasmic region of the HeLa cell and TEMPO-oxidized cellulose nanocrystals (TO-CNCs) conjugated with NH_2-CQD has better cytocompatibility.[31,89,90] While studying the bioimaging effect of biomass derived CQD on A549 cell, it is seen that it generally stains the cytoplasm of the A549 cell line with the difference in its luminance property depending upon different biomass derived CQDs, out of which the sugarcane bagasse derived CQDs and garlic derived CQDs gives better bioimaging of the cytosol compared to CQDs derived from coriander leaves, *Osmanthus Fragrans (Thunb.)*, rice-biryani (biowaste), corn stalk shell, fresh spinach, and lotus root.[43,91–97] Researchers have studied the bioimaging property of biomass derived CQD in various cells such as "LoVo cell, HepG2, MCF-7, MDA-MB 468,

MDA-MB-231, HaCaT, MC3T3, SiHa, HT-29, PC3, K-562, Hep3B, and MG-63 with different sources of biomass to design CQDs such as "Bee pollens, Peanuts, Peach gum polysaccharide, Tulsi leaves (Ocimum sanctum), P. Avium fruits, Carrots, Walnuts, Rose-heart radish, Watermelon juice, Quince fruit (Cydonia oblonga), Walnut oil, Fungus fibers, Allium fistulosum, Cyanobacteria, Rosa roxburghii, Lemon juice, Sandalwood-derived CQDs, Citrus fruit peels, Mexican mint, and *Aloe barbadensis miller* (Aloe vera) extract" and found that all of them broadly illuminate the cytoplasm region, suggesting a nonspecific bioimaging ability as it has not shown the property to tag specific cell organelles. The intensity of imaging changes according to the source of biomass.[24,26,29,34,35,44,98–110] It may be because of the different phytochemicals present in different biomass. Phytochemicals can play a major role in the fluorescent potential of a carbon dot was proved by a study done using different spices (cinnamon, red chilli, turmeric, black pepper) to synthesise CQDs by the same method and same parameters and found that the imaging property of each spice is different and we know spices are known for its phytochemical diversity. It was seen that the fluorescence quantum yields of cinnamon, red chilli, turmeric, and black pepper C-dots were high (35.7, 26.8, 38.3, and 43.6%, respectively), and the particle sizes were assessed by TEM to be 3.37, 3.14, 4.32, and 3.55 nm, respectively, which is well explained in Fig. 7.[111] It is seen that the biomass derived carbon dots generally stain the cytoplasmic region of the cell, but to date, no one has been able to design it in such a way that it can target the specific cell organelles. So further research must be done to specifically stain specific cell organelles.

6.2 *In vivo* imaging

The term *in vivo* means inside a living system. The importance of *in vivo* bioimaging is to detect the different abnormalities inside the body system, such as knowing the presence of cancerous cells, different hormones, proteins, and biochemicals. A carbon dot is made of carbon, which is biocompatible, low cytotoxic in nature, and so it is a potent product for *in vivo* bioimaging. Several scientists have worked in bioimaging, where they explored the potential of carbon dots to be a new alternative for nontoxic bioimaging substrates. In a study, it was established that carbon dots prepared from curcumin could detect the embryo of a zebrafish, and it was found that it is nontoxic to the zebrafish. Upon injecting, the CQDs were taken up by the 4-HPF embryo *via* the highly permeable chorionic membrane. Due to the chorionic membrane's selective character, the toxicity of embryos was lowered when compared to cell lines. The embryo treated with CQDs at $0.5~\mu g~mL^{-1}$ had a 52% survival rate. The zebrafish embryo is not significantly affected by the first low doses.[23] In the presence of CQDs prepared from *Gynostemma* at concentrations less than $400~\mu g~mL^{-1}$, the nervous and circulatory systems of zebrafish embryos developed normally.[113] Additionally, it is seen that the fluorescence in zebrafish embryos is primarily green, followed by blue, and the least in red. The end result is a superb display of CQDs in fluorescence imaging.[23] Zebrafish
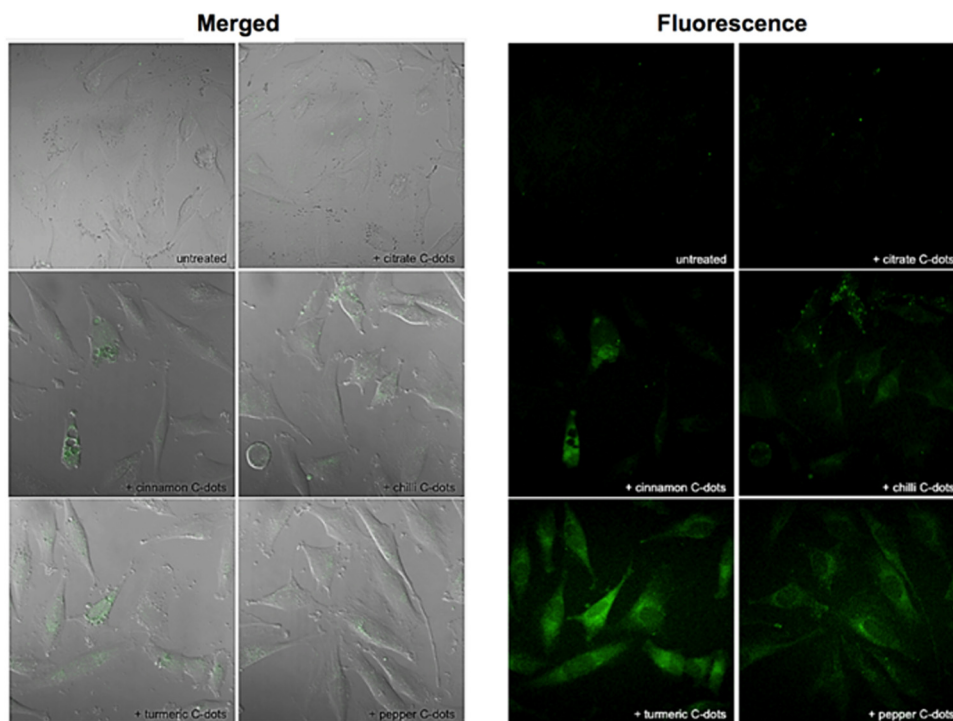
LN-229 cells

Fig. 7 After 24 h of incubation with either no C-dots (untreated) or with 1 mg mL^{-1} of citrate, cinnamon, red chilli, turmeric, and black pepper C-dots, the LN-229 cancer cells were imaged using combined transmission and fluorescence (left) and fluorescence (right) techniques. Using a 405 nm laser and a Zeiss LSM780 confocal microscope with a 40 objective, pictures were taken while capturing the green fluorescence that was emitted. Figure is reproduced from ref. 112 under Creative Common CC BY license, Copyright © 2018 Vasimalai *et al.*; licensee Beilstein-Institut.

embryos without CQDs did not show any fluorescence 2 h after fertilisation. On the contrary, after 22 h of incubation with CQDs, the embryos displayed intense fluorescence, indicating that CQDs may enter the embryos *via* the chorion.[113] Whereas glutathione rigidified reduced carbon quantum dots (r-CQDS) prepared from rice biryani waste showed a bright green and red

fluorescence throughout the body at 488 nm when it was injected in the tail vain of mice, as is shown in Fig. 8(A).[94] Because of their functionality, the biomass derived CQDs from banana peel exhibit strong fluorescence and an adequate quantum yield of 20% in water. They also have excellent water solubility. As great candidates for *in vivo* bioimaging
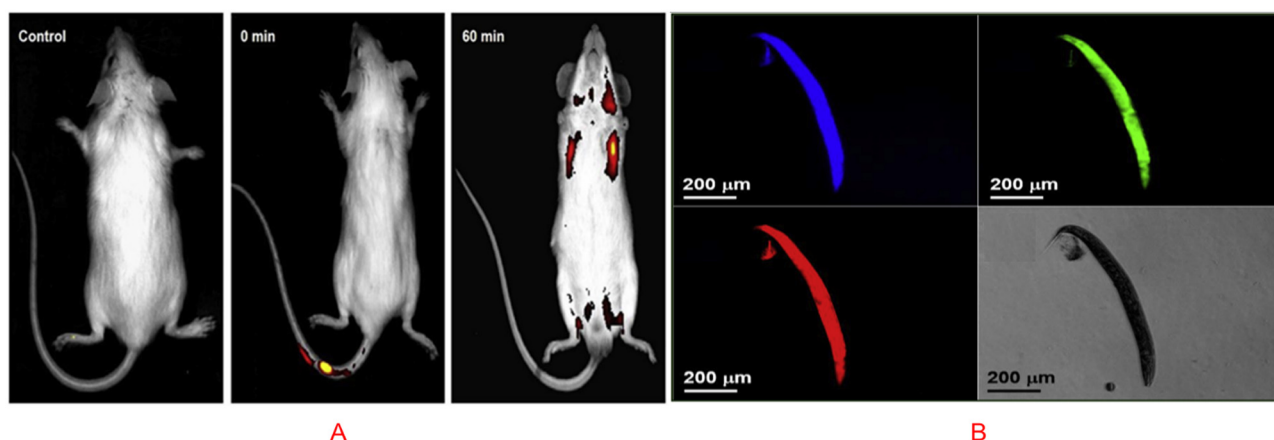

Fig. 8 (A) *In vivo* imaging with the entire body accumulating green r-CQDs-GS. One hour after receiving a tail vein injection, the total body fluorescent images show a higher accumulation of green r-CQDs-GS (488 nm), and the red to flaming yellow colour expressed a higher intensity of fluorescence. Figure is reproduced from ref. 94 under Copyright © 2019 Elsevier B.V. (B) N-CQDs made from *P. acidus* fruit incubated with *C. elegans* and imaged while under excitation. Figure is reproduced from ref. 115 under Copyright © 2018 Elsevier B.V.

applications, CQDs also exhibit outstanding fluorescence stability and good biocompatibility. Their excitation-dependent fluorescence characteristics have been successfully used in nematode multicolour imaging applications as a reliable fluorescent probe.[114] In another study, it was found that N-CQDs obtained from *P. adusci* fruits *via* the hydrothermal method were non-toxic and biocompatible. Biomass derived N-CQDs are promising optical/fluorescence nanoprobes for real-time live-cell imaging due to their excellent optical properties and good biocompatibility, as visualized in Fig. 8(B). Based on the different fluorescence filters, the N-CQDs were intensely stained and multiple fluorescences were uniformly distributed throughout the whole body of the nematodes.[115] By studying all the work done using biomass derived carbon dots, we can come to the conclusion that the biomass derived carbon dot is nontoxic and have efficient fluorescence activity for *in vivo* imaging. But the work done till now is not sufficient because we need to develop biomass derived carbon dots that can specifically target a specific biomolecule without interfering with the nearby biochemicals, which will in turn help us to detect different anomalies in the body.

7. Other applications of CQDs

Except bio-imaging, CQDs play a significant role in various fields of biomedical sciences like bioimaging, biosensors, nanomedicine, anticancer, tissue engineering, and drug delivery, as shown in Fig. 9. Exceptional physical, electrical, and electrochemical properties of CQDs enable them to act as sensing probes for biosensor applications. The versatile characteristics such as excitation dependent emission, enhanced photostability, less toxicity, and high-water solubility enable CQDs as a potential candidate for glucose, iron, phosphate, galactose, glucose, cystine, hydrogen peroxide, pH, and vitamin

Fig. 9 Schematic diagram depicting the biomedical applications of CQDs.

B_{12} sensing. In particular, CQDs are highly capable of adhering to the drug molecules *via* π–π interaction and bind the drug to the matrix. Ultra-small size of CQDs avails a significant surface area to encapsulate and load the drug molecules. The excellent fluorescent characteristics of CQDs help in tracing the drug delivery pathway similar to the conventional fluorescent dyes and semiconductor nanoparticles.

8. Conclusion and future outlook

Carbon quantum dots (C-dots, or CQDs) are a novel type of carbon nanomaterials with diameters below 10 nm. There are several methods for the synthesis of biomass derived carbon quantum dots, and every method has its own advantages. Comparing the ease of use and adaptability of hydrothermal and microwave-assisted synthesis techniques shows that between 180 °C and 200 °C, CQDs were hydrothermally created in 2–12 h. By lengthening the hydrothermal period, the carbonation at a lower temperature could be countered. Higher quantum yields were generally produced by chemicals with higher purity. Under microwave irradiation, the hydrothermal time could be reduced to 1 h; however, even with a closed vessel and subcritical temperatures, the quantum yield was not significantly increased. It is to be noted that organic acids like citric acid will increase the photo luminance property of the carbon dot, as we know that citric acid plays a major role when reacting with carbon dots to increase its fluorescent property. Due to quantum confinement effects, the size-dependent PL emission has been a notable feature in CQDs. For characteristic applications, tuning the shape and size is greatly desired, as the size, shape, and percentage of sp^2–sp^3 hybridised domains all affect the optical band gap of CQDs. Doping various metal or non-metal particles to the carbon dot may enhance the fluorescence property as well as it may turn it into target specific bioimaging tools. *In vitro* bioimaging, drug delivery, and photocatalysis are to be accomplished with the help of the synthesised CQDs due to their excellent photoinduced electron transfer, minimal cytotoxicity, and ability to harvest light efficiently. The carbon dot is used for various *in vitro* and *in vivo* imaging, where it targets the cytoplasmic region of the cell. Currently, CQD have been used to target various cells such as HELA and MCF7 under *in vitro* condition. In *in vivo* imaging, the CQD targets the organ as a whole but the effect of fluorescence can also be observed in the adjacent cells of the target organ. It is noted that if we design the carbon dots that can specifically target the cell organelles, then it would be a great success in the field of bioimaging as well as if we can design it in such a way that it can differentiate between live cells and dead cells. It will give us a great advantage to use a non-cytotoxic an inexpensive bioimaging material. Currently, the CQD is not particularly target specific when added alone but the addition of some metal or nonmetal may increase its specificity. Hence, we must try to develop the CQD in such a way that it only stains the specific target as well as target specific cell organelles. We can also see the role of various naturally occurring acids in the bioimaging property of CQD.
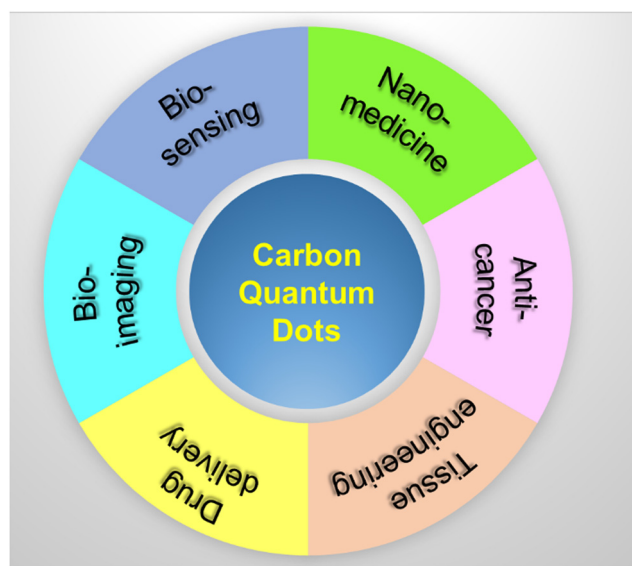
Conflicts of interest

There are no conflicts to declare.

References

1 N. S. Peighambardoust, E. Sadeghi and U. Aydemir, *ACS Appl. Nano Mater.*, 2022, **5**, 14092–14132.

2 C. R. Kagan, L. C. Bassett, C. B. Murray and S. M. Thompson, *Chem. Rev.*, 2021, **121**, 3186–3233.

3 D. Vasudevan, R. R. Gaddam, A. Trinchi and I. Cole, *J. Alloys Compd.*, 2015, **636**, 395–404.

4 D. A. Schwartz, N. S. Norberg, Q. P. Nguyen, J. M. Parker and D. R. Gamelin, *J. Am. Chem. Soc.*, 2003, **125**, 13205–13218.

5 R. Kottayi, D. K. Maurya, R. Sittaramane and S. Angaiah, *ES Energy Environ.*, 2022, **18**, 1–40.

6 S. E. Sheela, R. Sekar, D. K. Maurya, M. Paulraj and S. Angaiah, *Mater. Sci. Semicond. Process.*, 2023, **156**, 107273.

7 J. Liu, R. Li and B. Yang, *ACS Cent. Sci.*, 2020, **6**, 2179–2195.

8 W. Meng, X. Bai, B. Wang, Z. Liu, S. Lu and B. Yang, *Energy Environ. Mater.*, 2019, **2**, 172–192.

9 J. Zhang and S.-H. Yu, *Mater. Today*, 2016, **19**, 382–393.

10 P. G. Luo, S. Sahu, S.-T. Yang, S. K. Sonkar, J. Wang, H. Wang, G. E. LeCroy, L. Cao and Y.-P. Sun, *J. Mater. Chem. B*, 2013, **1**, 2116–2127.

11 N. Tejwan, S. K. Saha and J. Das, *Adv. Colloid Interface Sci.*, 2020, **275**, 102046.

12 V. Sharma, P. Tiwari and S. M. Mobin, *J. Mater. Chem. B*, 2017, **5**, 8904–8924.

13 Z. Kang and S.-T. Lee, *Nanoscale*, 2019, **11**, 19214–19224.

14 C. Ji, Y. Zhou, R. M. Leblanc and Z. Peng, *ACS Sens.*, 2020, **5**, 2724–2741.

15 W. Meng, B. Wang, L. Ai, H. Song and S. Lu, *J. Colloid Interface Sci.*, 2021, **598**, 274–282.

16 P. Bag, R. K. Maurya, A. Dadwal, M. Sarkar, P. A. Chawla, R. K. Narang and B. Kumar, *ChemistrySelect*, 2021, **6**, 2774–2789.

17 S. D. Torres Landa, N. K. Reddy Bogireddy, I. Kaur, V. Batra and V. Agarwal, *iScience*, 2022, **25**, 103816.

18 Y. Wang, J. Sun, B. He and M. Feng, *Green Chem. Eng.*, 2020, **1**, 94–108.

19 M. Fang, B. Wang, X. Qu, S. Li, J. Huang, J. Li, S. Lu and N. Zhou, *Chin. Chem. Lett.*, 2023, 108423.

20 W. Li, Y. Liu, B. Wang, H. Song, Z. Liu, S. Lu and B. Yang, *Chin. Chem. Lett.*, 2019, **30**, 2323–2327.

21 B. Domingo-Tafalla, E. Martínez-Ferrero, F. Franco and E. Palomares-Gil, *Molecules*, 2022, **27**, 1081.

22 B. D. Mansuriya and Z. Altintas, *Nanomaterials*, 2021, **11**, 2525.

23 T. Pal, S. Mohiyuddin and G. Packirisamy, *ACS Omega*, 2018, **3**, 831–843.

24 V. Roshni, S. Misra, M. K. Santra and D. Ottoor, *J. Photochem. Photobiol., A*, 2019, **373**, 28–36.

25 K. Rajendran, G. Rajendran, J. Kasthuri, K. Kathiravan and N. Rajendiran, *ChemistrySelect*, 2019, **4**, 13668–13676.

26 A. Tadesse, M. Hagos, D. RamaDevi, K. Basavaiah and N. Belachew, *ACS Omega*, 2020, **5**, 3889–3898.

27 N. R. Pires, C. M. W. Santos, R. R. Sousa, R. C. M. D. Paula, P. L. R. Cunha and J. P. A. Feitosa, *J. Braz. Chem. Soc.*, 2015, **26**, 1274–1282.

28 N. Sharma, I. Sharma and M. K. Bera, *J. Fluoresc.*, 2022, **32**, 1032–1049.

29 N. Architha, M. Ragupathi, C. Shobana, T. Selvankumar, P. Kumar, Y. S. Lee and R. Kalai Selvan, *Environ. Res.*, 2021, **199**, 111263.

30 M. L. Desai, S. Jha, H. Basu, R. K. Singhal, T.-J. Park and S. K. Kailasa, *ACS Omega*, 2019, **4**, 19332–19340.

31 J. Zhou, Z. Sheng, H. Han, M. Zou and C. Li, *Mater. Lett.*, 2012, **66**, 222–224.

32 M. Xue, M. Zou, J. Zhao, Z. Zhan and S. Zhao, *J. Mater. Chem. B*, 2015, **3**, 6783–6789.

33 M. Xue, J. Zhao, Z. Zhan, S. Zhao, C. Lan, F. Ye and H. Liang, *Nanoscale*, 2018, **10**, 18124–18130.

34 M. Xue, Z. Zhan, M. Zou, L. Zhang and S. Zhao, *New J. Chem.*, 2016, **40**, 1698–1703.

35 D. Shukla, M. Das, D. Kasade, M. Pandey, A. K. Dubey, S. K. Yadav and A. S. Parmar, *Chemosphere*, 2020, **248**, 125998.

36 R. Meena, R. Singh, G. Marappan, G. Kushwaha, N. Gupta, R. Meena, J. P. Gupta, R. R. Agarwal, N. Fahmi and O. S. Kushwaha, *Heliyon*, 2019, **5**, e02483.

37 J. Singh, S. Kaur, J. Lee, A. Mehta, S. Kumar, K.-H. Kim, S. Basu and M. Rawat, *Sci. Total Environ.*, 2020, **720**, 137604.

38 N. Sharma, I. Sharma and M. K. Bera, *J. Fluoresc.*, 2022, **32**, 1039–1049.

39 T. Arumugham, M. Alagumuthu, R. G. Amimodu, S. Munusamy and S. K. Iyer, *Sustainable Mater. Technol.*, 2020, **23**, e00138.

40 Y. Ran, S. Wang, Q. Yin, A. Wen, X. Peng, Y. Long and S. Chen, *Luminescence*, 2020, **35**, 870–876.

41 J. Athinarayanan, V. S. Periasamy and A. A. Alshatwi, *ACS Omega*, 2022, **7**, 19270–19279.

42 K. Rajendran, G. Rajendran, J. Kasthuri, K. Kathiravan and N. Rajendiran, *ChemistrySelect*, 2019, **4**, 13668–13676.

43 A. Sachdev and P. Gopinath, *Analyst*, 2015, **140**, 4260–4269.

44 Z. Ramezani, M. Qorbanpour and N. Rahbar, *Colloids Surf., A*, 2018, **549**, 58–66.

45 J. R. Bhamore, S. Jha, T. J. Park and S. K. Kailasa, *J. Photochem. Photobiol., B*, 2019, **191**, 150–155.

46 N. Azam, M. Najabat Ali and T. Javaid Khan, *Front. Mater.*, 2021, **8**, DOI: 10.3389/fmats.2021.700403/full.

47 G. Ayiloor Rajesh, V. L. John, A. Pookunnath Santhosh, A. Krishnan Nair Ambika and V. Thavarool Puthiyedath, *Part. Part. Syst. Charact.*, 2022, **39**, 2200017.

48 H. R. A. K. Al-Hetty, A. T. Jalil, J. H. Z. Al-Tamimi, H. G. Shakier, M. Kandeel, M. M. Saleh and M. Naderifar, *Inorg. Chem. Commun.*, 2023, **149**, 110433.

49 S. Sikiru, T. L. Oladosu, S. Y. Kolawole, L. A. Mubarak, H. Soleimani, L. O. Afolabi and A.-O. Oluwafunke Toyin, *J. Energy Storage*, 2023, **60**, 106556.

50 K. Naik, S. Chaudhary, L. Ye and A. S. Parmar, *Front. Bioeng. Biotechnol.*, 2022, **10**, DOI: 10.3389/fbioe.2022.882100.

51 H. H. Jing, F. Bardakci, S. Akgöl, K. Kusat, M. Adnan, M. J. Alam, R. Gupta, S. Sahreen, Y. Chen, S. C. B. Gopinath and S. Sasidharan, *Chem. Commun.*, 2023, **14**, 27.

52 M. E. Khan, A. Mohammad and T. Yoon, *Chemosphere*, 2022, **302**, 134815.

53 L. Cui, X. Ren, M. Sun, H. Liu and L. Xia, *Nanomaterials*, 2021, **11**, 3419.

54 D. Qu and Z. Sun, *Mater. Chem. Front.*, 2020, **4**, 400–420.

55 J. Wang, R. S. Li, H. Z. Zhang, N. Wang, Z. Zhang and C. Z. Huang, *Biosens. Bioelectron.*, 2017, **97**, 157–163.

56 J. Jana, H. J. Lee, J. S. Chung, M. H. Kim and S. H. Hur, *Anal. Chim. Acta*, 2019, **1079**, 212–219.

57 J. Hu, F. Tang, Y.-Z. Jiang and C. Liu, *Analyst*, 2020, **145**, 2184–2190.

58 V. Raveendran and R. N. Kizhakayil, *ACS Omega*, 2021, **6**, 23475–23484.

59 M. L. Liu, B. B. Chen, C. M. Li and C. Z. Huang, *Green Chem.*, 2019, **21**, 449–471.

60 K. Qin, D. Zhang, Y. Ding, X. Zheng, Y. Xiang, J. Hua, Q. Zhang, X. Ji, B. Li and Y. Wei, *Analyst*, 2020, **145**, 177–183.

61 L. Cui, J. Wang and M. Sun, *Rev. Phys.*, 2021, **6**, 100054.

62 W. Meng, X. Bai, B. Wang, Z. Liu, S. Lu and B. Yang, *Energy Environ. Mater.*, 2019, **2**, 172–192.

63 G. S. Das, J. P. Shim, A. Bhatnagar, K. M. Tripathi and T. Kim, *Sci. Rep.*, 2019, **9**, 15084.

64 C. Dias, N. Vasimalai, M. P. Sárria, I. Pinheiro, V. Vilas-Boas, J. Peixoto and B. Espiña, *Nanomaterials*, 2019, **9**, 199.

65 Y. Wang, P. Anilkumar, L. Cao, J.-H. Liu, P. G. Luo, K. N. Tackett, S. Sahu, P. Wang, X. Wang and Y.-P. Sun, *Exp. Biol. Med.*, 2011, **236**, 1231–1238.

66 W. Wang, Y. Li, L. Cheng, Z. Cao and W. Liu, *J. Mater. Chem. B*, 2014, **2**, 46–48.

67 F. Ostadhossein and D. Pan, *Wiley Interdiscip. Rev.: Nanomed. Nanobiotechnol.*, 2017, **9**, e1436.

68 W. Denk, J. H. Strickler and W. W. Webb, *Science*, 1990, **248**, 73–76.

69 L. Cao, X. Wang, M. J. Meziani, F. Lu, H. Wang, P. G. Luo, Y. Lin, B. A. Harruff, L. M. Veca, D. Murray, S.-Y. Xie and Y.-P. Sun, *J. Am. Chem. Soc.*, 2007, **129**, 11318–11319.

70 B. Wang, Y. Wang, H. Wu, X. Song, X. Guo, D. Zhang, X. Ma and M. Tan, *RSC Adv.*, 2014, **4**, 49960–49963.

71 B. Kong, A. Zhu, C. Ding, X. Zhao, B. Li and Y. Tian, *Adv. Mater.*, 2012, **24**, 5844–5848.

72 E. Hemmer, A. Benayas, F. Légaré and F. Vetrone, *Nanoscale Horiz.*, 2016, **1**, 168–184.

73 J. Qi, C. Sun, D. Li, H. Zhang, W. Yu, A. Zebibula, J. W. Y. Lam, W. Xi, L. Zhu, F. Cai, P. Wei, C. Zhu, R. T. K. Kwok, L. L. Streich, R. Prevedel, J. Qian and B. Z. Tang, *ACS Nano*, 2018, **12**, 7936–7945.

74 D. Li, D. Wang, X. Zhao, W. Xi, A. Zebibula, N. Alifu, J.-F. Chen and J. Qian, *Mater. Chem. Front.*, 2018, **2**, 1343–1350.

75 D. Li, P. Jing, L. Sun, Y. An, X. Shan, X. Lu, D. Zhou, D. Han, D. Shen, Y. Zhai, S. Qu, R. Zbořil and A. L. Rogach, *Adv. Mater.*, 2018, **30**, 1705913.

76 A. Zhao, Z. Chen, C. Zhao, N. Gao, J. Ren and X. Qu, *Carbon*, 2015, **85**, 309–327.

77 N. Li, X. Liang, L. Wang, Z. Li, P. Li, Y. Zhu and J. Song, *J. Nanopart. Res.*, 2012, **14**, 1177.

78 G. H. G. Ahmed, R. B. Laíño, J. A. G. Calzón and M. E. D. García, *Talanta*, 2015, **132**, 252–257.

79 M. Havrdova, K. Hola, J. Skopalik, K. Tomankova, M. Petr, K. Cepe, K. Polakova, J. Tucek, A. B. Bourlinos and R. Zboril, *Carbon*, 2016, **99**, 238–248.

80 C. Y. Chung, Y. J. Chen, C. H. Kang, H. Y. Lin, C. C. Huang, P. H. Hsu and H. J. Lin, *Polymers*, 2021, **13**, 1598.

81 N. Malik, T. Arfin and A. U. Khan, in *Nanomaterials for Drug Delivery and Therapy*, ed. A. M. Grumezescu, William Andrew Publishing, 2019, pp. 373–402.

82 S. M. Hickey, B. Ung, C. Bader, R. Brooks, J. Lazniewska, I. R. D. Johnson, A. Sorvina, J. Logan, C. Martini, C. R. Moore, L. Karageorgos, M. J. Sweetman and D. A. Brooks, *Cells*, 2021, **11**, 35.

83 J. Niu, X. Wang, J. Lv, Y. Li and B. Tang, *TrAC, Trends Anal. Chem.*, 2014, **58**, 112–119.

84 J. Shen, Y. Zhu, X. Yang and C. Li, *Chem. Commun.*, 2012, **48**, 3686–3699.

85 H. Li, Z. Kang, Y. Liu and S.-T. Lee, *J. Mater. Chem.*, 2012, **22**, 24230–24253.

86 K. Hola, Y. Zhang, Y. Wang, E. P. Giannelis, R. Zboril and A. L. Rogach, *Nano Today*, 2014, **9**, 590–603.

87 X. Li, M. Rui, J. Song, Z. Shen and H. Zeng, *Adv. Funct. Mater.*, 2015, **25**, 4929–4947.

88 X. T. Zheng, A. Ananthanarayanan, K. Q. Luo and P. Chen, *Small*, 2015, **11**, 1620–1636.

89 J. Guo, D. Liu, I. Filpponen, L.-S. Johansson, J.-M. Malho, S. Quraishi, F. Liebner, H. A. Santos and O. J. Rojas, *Biomacromolecules*, 2017, **18**, 2045–2055.

90 Y. Wan, M. Wang, K. Zhang, Q. Fu, M. Gao, L. Wang, Z. Xia and D. Gao, *Microchem. J.*, 2019, **148**, 385–396.

91 F. Du, M. Zhang, X. Li, J. Li, X. Jiang, Z. Li, Y. Hua, G. Shao, J. Jin, Q. Shao, M. Zhou and A. Gong, *Nanotechnology*, 2014, **25**, 315702.

92 L. Li, R. Zhang, C. Lu, J. Sun, L. Wang, B. Qu, T. Li, Y. Liu and S. Li, *J. Mater. Chem. B*, 2017, **5**, 7328–7334.

93 Z. Li, Q. Wang, Z. Zhou, S. Zhao, S. Zhong, L. Xu, Y. Gao and X. Cui, *Microchem. J.*, 2021, **166**, 106250.

94 A. M. Anthony, R. Murugan, R. Subramanian, G. K. Selvarangan, P. Pandurangan, A. Dhanasekaran and A. Sohrab, *Colloids Surf., A*, 2020, **586**, 124266.

95 M. Wang, Y. Wan, K. Zhang, Q. Fu, L. Wang, J. Zeng, Z. Xia and D. Gao, *Anal. Bioanal. Chem.*, 2019, **411**, 2715–2727.

96 S. Zhao, M. Lan, X. Zhu, H. Xue, T.-W. Ng, X. Meng, C.-S. Lee, P. Wang and W. Zhang, *ACS Appl. Mater. Interfaces*, 2015, **7**, 17054–17060.

97 D. Gu, S. Shang, Q. Yu and J. Shen, *Appl. Surf. Sci.*, 2016, **390**, 38–42.

98 J. Liao, Z. Cheng and L. Zhou, *ACS Sustainable Chem. Eng.*, 2016, **4**, 3053–3061.

99 J. Zhang, Y. Yuan, G. Liang and S.-H. Yu, *Adv. Sci.*, 2015, **2**, 1500002.

100 A. Kumar, A. R. Chowdhuri, D. Laha, T. K. Mahto, P. Karmakar and S. K. Sahu, *Sens. Actuators, B*, 2017, **242**, 679–686.

101 T. N. J. I. Edison, R. Atchudan, J.-J. Shim, S. Kalimuthu, B.-C. Ahn and Y. R. Lee, *J. Photochem. Photobiol., B*, 2016, **158**, 235–242.

102 C. Cheng, Y. Shi, M. Li, M. Xing and Q. Wu, *Mater. Sci. Eng.: C*, 2017, **79**, 473–480.

103 W. Liu, H. Diao, H. Chang, H. Wang, T. Li and W. Wei, *Sens. Actuators, B*, 2017, **241**, 190–198.

104 M. Lu, Y. Duan, Y. Song, J. Tan and L. Zhou, *J. Mol. Liq.*, 2018, **269**, 766–774.

105 C. Shi, H. Qi, R. Ma, Z. Sun, L. Xiao, G. Wei, Z. Huang, S. Liu, J. Li, M. Dong, J. Fan and Z. Guo, *Mater. Sci. Eng.: C*, 2019, **105**, 110132.

106 E. Arkan, A. Barati, M. Rahmanpanah, L. Hosseinzadeh, S. Moradi and M. Hajialyani, *Adv. Pharm. Bull.*, 2018, **8**, 149–155.

107 Z. Wei, B. Wang, Y. Liu, Z. Liu, H. Zhang, S. Zhang, J. Chang and S. Lu, *New J. Chem.*, 2019, **43**, 718–723.

108 Q. Zhang, J. Liang, L. Zhao, Y. Wang, Y. Zheng, Y. Wu and L. Jiang, *Front. Chem.*, 2020, **8**, DOI: 10.3389/fchem.2020.00665.

109 X. Wang, P. Yang, Q. Feng, T. Meng, J. Wei, C. Xu and J. Han, *Polymers*, 2019, **11**, 616.

110 J. P. Malavika, C. Shobana, M. Ragupathi, P. Kumar, Y. S. Lee, M. Govarthanan and R. K. Selvan, *Environ. Res.*, 2021, **200**, 111414.

111 N. Vasimalai, V. Vilas-Boas, J. Gallo, M. de Fátima Cerqueira, M. Menéndez-Miranda, J. M. Costa-Fernández, L. Diéguez, B. Espiña and M. T. Fernández-Argüelles, *Beilstein J. Nanotechnol.*, 2018, **9**, 530–544.

112 N. Vasimalai, V. Vilas-Boas, J. Gallo, M. D. F. Cerqueira, M. Menéndez-Miranda, J. M. Costa-Fernández, L. Diéguez, B. Espiña and M. T. Fernández-Argüelles, *Beilstein J. Nanotechnol.*, 2018, **9**, 530–544.

113 X. Wei, L. Li, J. Liu, L. Yu, H. Li, F. Cheng, X. Yi, J. He and B. Li, *ACS Appl. Mater. Interfaces*, 2019, **11**, 9832–9840.

114 R. Atchudan, T. N. Jebakumar Immanuel Edison, M. Shanmugam, S. Perumal, T. Somanathan and Y. R. Lee, *Phys. E*, 2021, **126**, 114417.

115 R. Atchudan, T. N. J. I. Edison, S. Perumal, N. Clament Sagaya Selvam and Y. R. Lee, *J. Photochem. Photobiol., A*, 2019, **372**, 99–107.